

## Selective Etching of Graphene Edges by Hydrogen Plasma

Liming Xie, Liying Jiao, and Hongjie Dai\*

Department of Chemistry, Stanford University, Stanford, California 94305

Received August 6, 2010; E-mail: hdai1@stanford.edu

**Abstract:** We devised a controlled hydrogen plasma reaction at 300 °C to etch graphene and graphene nanoribbons (GNRs) selectively at the edges over the basal plane. Atomic force microscope imaging showed that the etching rates for single-layer and few-layer ( $\geq 2$  layers) graphene are  $0.27 \pm 0.05$  nm/min and  $0.10 \pm 0.03$  nm/min, respectively. Meanwhile, Raman spectroscopic mapping revealed no D band in the planes of single-layer or few-layer graphene after the plasma reaction, suggesting selective etching at the graphene edges without introducing defects in the basal plane. We found that hydrogen plasma at lower temperature (room temperature) or a higher temperature (500 °C) could hydrogenate the basal plane or introduce defects in the basal plane. Using the hydrogen plasma reaction at the intermediate temperature (300 °C), we obtained narrow, presumably hydrogen terminated GNRs (sub-5 nm) by etching of wide GNRs derived from unzipping of multiwalled carbon nanotubes. Such GNRs exhibited semiconducting characteristics with high on/off ratios ( $\sim 1000$ ) in GNR field effect transistor devices at room temperature.

Graphene has attracted much interest in recent years as a novel material for fundamental physics<sup>1–3</sup> and potential applications.<sup>4–6</sup> For nanoelectronics applications, narrow graphene nanoribbons (GNRs) with widths  $< \sim 5$  nm are needed to exhibit semiconducting characteristics with sufficiently large band gaps for high on/off transistor operations.<sup>7–9</sup> Several methods have been developed to fabricate or synthesize GNRs.<sup>10–15</sup> Lithographic patterning<sup>15</sup> can produce GNRs with widths  $> 20$  nm. Sonication of graphene sheets<sup>13</sup> and unzipping of carbon nanotubes (CNTs)<sup>10,11</sup> have yielded GNRs with widths down to sub-5 nm.<sup>10,16</sup> Recently, controlled gas-phase oxidation at  $\sim 800$  °C was developed to selectively etch the edges of GNRs for narrowing down to sub-5 nm<sup>17</sup> and producing semiconducting GNR devices with high on/off electrical switching. Also recently, there have been reports of anisotropic etching of graphene starting from sites in the plane and at the edges of graphene.<sup>18,19</sup>

Much room exists for exploring lower temperature reactions for selective etching of one-layer and few-layer graphene at the edges without damaging the basal plane. Further, it is desirable to control the chemical termination of the edges of graphene sheets and GNRs due to their profound effect on the physical properties of GNRs.<sup>20,21</sup> For instance, hydrogen termination of graphene and GNRs has been widely predicted to be useful for spintronics applications.<sup>20,22</sup> It is established that hydrogen plasma can hydrogenate<sup>23,24</sup> and etch<sup>25,26</sup> graphite and graphene. Although theoretically proposed,<sup>27</sup> it remains unclear if a hydrogen plasma reaction condition can be devised for selective reactions with the graphene edges without etching or introducing defects in its basal plane. Here, we present a 300 °C hydrogen plasma reaction that achieves this goal for graphene sheets with various layer numbers including monolayer graphene. The

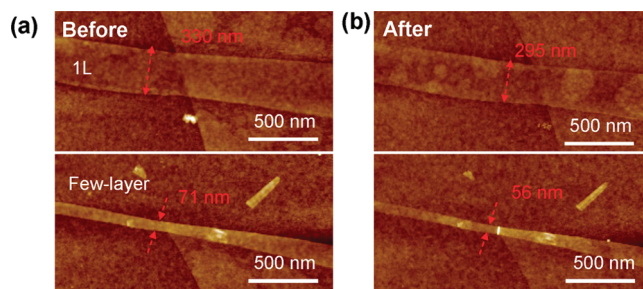


**Figure 1.** AFM images of two small pieces of graphene [top: a monolayer (1 L) graphene strip; bottom: a few-layer graphene strip] (a) before and (b) after selective hydrogen plasma edge etching for 60 min at 300 °C.

reaction was used to etch GNRs from the edges to produce semiconducting GNRs that are presumably H-terminated at the edges.

A hydrogen plasma reaction was performed for various times in a home-built remote plasma system [(see Supporting Information (SI) for experimental details)] at 300 °C under a hydrogen pressure of 300 mTorr. A plasma power of  $\sim 20$  W was used. The distance between graphene/GNR samples and the plasma source was kept at 40 cm, avoiding direct exposure of graphene to the plasma.

Figure 1a shows AFM images of as-made monolayer (1 L, identified by Raman spectroscopy<sup>28,29</sup> as in Figure S2) graphene and few-layer ( $\sim 2$  L or 3 L, AFM height of 1.2 nm) graphene. The layer number of few-layer graphene was identified by AFM topographic height measurement.<sup>28</sup> The initial widths of the 1 L graphene strip and few-layer graphene strip were  $\sim 330$  and  $\sim 71$  nm, respectively. After 60 min of hydrogen plasma treatment, the graphene strips were reduced to  $\sim 295$  and  $\sim 56$  nm (Figure 1b), corresponding to etching rates of 0.29 and 0.12 nm/min, respectively. Etching experiments of four different chips in four independent runs under the same plasma conditions found etching rates of  $0.27 \pm 0.05$  nm/min for 1 L graphene and  $0.10 \pm 0.03$  nm/min for few-layer ( $\geq 2$  L) graphene.

No apparent etching or hole formation was observed in the plane of graphene by AFM, suggesting selective hydrogen plasma etching at the graphene edges. To confirm this finding, Raman spectroscopic mapping was performed on large graphene sheets before and after plasma treatment. Figure 2a shows an AFM image of a large piece of graphene sheet, for which Raman mapping was used again to identify the layer numbers (see Figure S2). Figure 2b and 2c show the G band mapping and D band mapping of the graphene, respectively. Before reaction, the disorder related D band was only observed on the edges of graphene but not in the plane, suggesting the high-quality pristine nature of the graphene sheet. After 60 min of plasma treatment under the same conditions as in the experiment in Figure 1, Raman mapping detected a similar D band at the edges of the sheet as in the case before the reaction, but still no obvious D band was detected in the graphene plane including in all of the 1 L, bilayer (2 L), and multilayer (ML) regions. This suggested

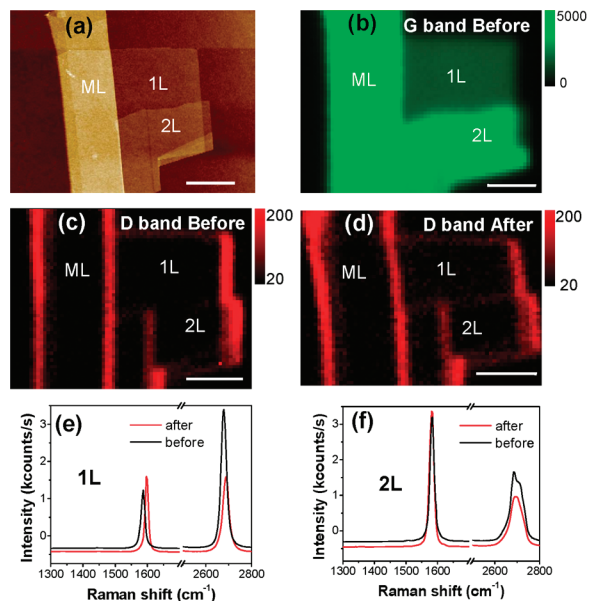


**Figure 2.** (a) AFM images of a large piece of graphene containing monolayer (1 L), bilayer (2 L), and multilayer (ML) regions. (b) G band mapping and (c) D band mapping of the graphene before plasma treatment. (d) D band mapping after 60 min of 300 °C hydrogen plasma treatment. Raman spectra of (e) the 1 L region and (f) the 2 L region before and after the reaction. The scale bars in (a)–(d) are 2  $\mu\text{m}$ .

that while etching at the graphene edges was occurring at a rate of 0.1–0.3 nm/min (Figure 1), no hydrogenation or related defect was created in the plane of graphene through the plasma treatment under our mild reaction conditions. This confirmed the high selectivity of hydrogen plasma etching at the graphene edge over the basal plane. The Raman frequency shift and 2D (or G') intensity decrease after plasma treatment (Figure 2e–f) may due to a vacuum annealing effect (see SI).

Hydrogen plasma has been used to hydrogenate graphene in the plane at room temperature (RT).<sup>23,24</sup> In-plane hydrogenation of graphene did not occur in our reaction since the reaction condition was controlled by the low plasma power, high pressure of  $\text{H}_2$ , and long distance from the graphene sample location to the plasma source. Also important is that in-plane hydrogenation of pristine graphene is thermodynamically energetic, and the reverse dehydrogenation reaction can occur at 300 °C.<sup>23</sup> We performed a control experiment treating graphene with the same plasma at RT (see SI), after which a weak D band was observed in the basal plane of 1 L graphene (not on 2 L, Figure S3), in agreement with the prior result.<sup>24</sup> Since no D band was observed in the plane of 1 L graphene (known to be more reactive than  $\geq 2$  L graphene) for 300 °C plasma treatment, the results suggest that the 300 °C hydrogen plasma reaction condition was milder than the RT reaction. This was attributed to the increased dehydrogenation at high temperatures. At an even higher temperature of 500 °C, however, we found similar D bands in the plane of 1 L graphene for the RT reaction (Figure S4), likely due to the much increased hydrogenation rate of in-plane carbon atoms at 500 °C against thermal dehydrogenation. These results suggested that the selective etching of 1 L graphene by hydrogen plasma is preferred at an intermediate temperature of around 300 °C.

Etching at graphene edges by hydrogen plasma may involve two steps.<sup>30,31</sup> Since carbon atoms at the graphene edges are more reactive, the first step could be hydrogenation of carbon atoms at the edges by reactive H species in the plasma to form C–H groups. These edge groups are more stable than in-plane C–H groups.<sup>27</sup>

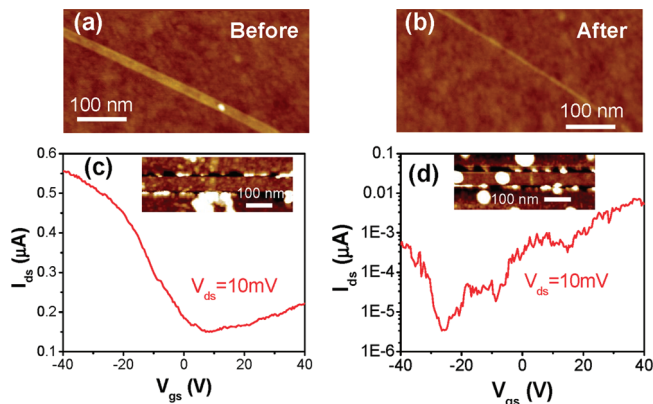


**Figure 3.** AFM images of a GNR (a) before and (b) after hydrogen plasma for 55 min. Room-temperature curves of drain–source current ( $I_{\text{ds}}$ ) to gate–source voltage ( $V_{\text{gs}}$ ) of (c) a GNR (width of  $\sim 14$  nm) device and (d) a plasma-narrowed GNR (width  $< 5$  nm) device. The insets are the AFM images of the corresponding devices.

The C–C bonds adjacent to the edge C–H groups could be cleaved subsequently and form new C–H bonds due to further hydrogenation, with the release of  $\text{CH}_4$  species. This hydrogenation and etching cycle may continue to remove C atoms from the edges. At the end of the reaction, the edges of graphene are presumably terminated by hydrogen.

Selective hydrogen plasma etching of graphene at the edges can be used to etch wide GNRs into sub-5 nm semiconductors without creating defects in the plane of the GNR. An initially  $\sim 14$  nm wide GNR (Figure 3a) was narrowed down to less than 5 nm (Figures 3b and S5) by this method and made into a field-effect transistor (FET) device on  $\text{SiO}_2/\text{Si}$  with Pd as the source/drain contact metal and Si substrate as the back gate. Without narrowing,  $\sim 14$  nm wide GNRs exhibited metallic characteristics with on/off ratios of only  $\sim 2$ –5 (Figure 3c).<sup>12</sup> The narrowed GNR exhibited an on/off ratio up to  $\sim 1000$  in the source–drain current vs gate voltage ( $I_{\text{ds}} - V_{\text{gs}}$ ) transfer characteristics (Figure 3d), suggesting a band gap opening.

In summary, we devised a controlled hydrogen plasma reaction at 300 °C to selectively etch graphene from edges without hydrogenating the graphene plane. We used this etching method to obtain semiconducting GNRs with less than a 5 nm width. This reaction may prove useful for tuning the size of graphene and affording hydrogen termination useful for spintronics applications.

**Acknowledgment.** We thank J. McVittie for help with the plasma system. This work was supported by Intel, MARCO-MSD, Graphene MURI, NSF CHE-0639053, and ONR.

**Supporting Information Available:** Setup of home-built plasma system, experimental details, Raman assignment of graphene layer numbers, possible explanation for Raman shift after plasma treatment, Raman spectra of RT hydrogen plasma treated graphene, Raman spectra of 500 °C hydrogen plasma treated graphene, and width measurement of the narrowed GNR in Figure 3b. This material is available free of charge via the Internet at <http://pubs.acs.org>.

## References

- (1) Nair, R. R.; Blake, P.; Grigorenko, A. N.; Novoselov, K. S.; Booth, T. J.; Stauber, T.; Peres, N. M. R.; Geim, A. K. *Science* **2008**, 320 (5881), 1308–1308.
- (2) Novoselov, K. S.; Geim, A. K.; Morozov, S. V.; Jiang, D.; Katsnelson, M. I.; Grigorieva, I. V.; Dubonos, S. V.; Firsov, A. A. *Nature* **2005**, 438 (7065), 197–200.
- (3) Cresti, A.; Nemec, N.; Biel, B.; Niebler, G.; Triozon, F.; Cuniberti, G.; Roche, S. *Nano Res.* **2008**, 1 (5), 361–394.

- (4) Yoo, E.; Okata, T.; Akita, T.; Kohyama, M.; Nakamura, J.; Honma, I. *Nano Lett.* **2009**, 9 (6), 2255–2259.
- (5) Zhang, H.; Bao, Q. L.; Tang, D. Y.; Zhao, L. M.; Loh, K. *Appl. Phys. Lett.* **2009**, 95 (14), 141103.
- (6) Xie, L. M.; Ling, X.; Fang, Y.; Zhang, J.; Liu, Z. F. *J. Am. Chem. Soc.* **2009**, 131 (29), 9890–9891.
- (7) Son, Y. W.; Cohen, M. L.; Louie, S. G. *Phys. Rev. Lett.* **2006**, 97 (21), 216803.
- (8) Wu, X. J.; Zeng, X. C. *Nano Res.* **2008**, 1 (1), 40–45.
- (9) Barone, V.; Hod, O.; Scuseria, G. E. *Nano Lett.* **2006**, 6 (12), 2748–2754.
- (10) Jiao, L. Y.; Zhang, L.; Wang, X. R.; Diankov, G.; Dai, H. J. *Nature* **2009**, 458 (7240), 877–880.
- (11) Kosynkin, D. V.; Higginbotham, A. L.; Sinitskii, A.; Lomeda, J. R.; Dimiev, A.; Price, B. K.; Tour, J. M. *Nature* **2009**, 458 (7240), 872–U5.
- (12) Jiao, L. Y.; Wang, X. R.; Diankov, G.; Wang, H. L.; Dai, H. J. *Nat. Nanotechnol.* **2010**, 5 (5), 321–325.
- (13) Wu, Z. S.; Ren, W. C.; Gao, L. B.; Liu, B. L.; Zhao, J. P.; Cheng, H. M. *Nano Res.* **2010**, 3 (1), 16–22.
- (14) Li, X. L.; Wang, X. R.; Zhang, L.; Lee, S. W.; Dai, H. J. *Science* **2008**, 319 (5867), 1229–1232.
- (15) Han, M. Y.; Ozyilmaz, B.; Zhang, Y. B.; Kim, P. *Phys. Rev. Lett.* **2007**, 98 (20), 206805.
- (16) Jiao, L. Y.; Zhang, L.; Ding, L.; Liu, J. E.; Dai, H. J. *Nano Res.* **2010**, 3 (6), 387–394.
- (17) Wang, X. R.; Dai, H. J. *Nat. Chem.* **2010**, (2), 661–665.
- (18) Nemes-Incze, P.; Magda, G.; Kamaras, K.; Biro, L. P. *Nano Res.* **2010**, 3 (2), 110–116.
- (19) Rong, Y.; Zhang, L.; Wang, Y.; Shi, Z.; Shi, D.; Gao, H.; Wang, E.; Zhang, G. *Adv. Mater.* **2010**, 22, 4014–4019.
- (20) Cantele, G.; Lee, Y. S.; Ninno, D.; Marzari, N. *Nano Lett.* **2009**, 9 (10), 3425–3429.
- (21) Cervantes-Sodi, F.; Csanyi, G.; Piscanec, S.; Ferrari, A. C. *Phys. Rev. B* **2008**, 77 (16), 165427.
- (22) Bhandary, S.; Eriksson, O.; Biplab, S. arXiv:1005.5714v1, 2010.
- (23) Luo, Z. Q.; Yu, T.; Kim, K. J.; Ni, Z. H.; You, Y. M.; Lim, S.; Shen, Z. X.; Wang, S. Z.; Lin, J. Y. *ACS Nano* **2009**, 3 (7), 1781–1788.
- (24) Elias, D. C.; Nair, R. R.; Mohiuddin, T. M. G.; Morozov, S. V.; Blake, P.; Halsall, M. P.; Ferrari, A. C.; Boukhvalov, D. W.; Katsnelson, M. I.; Geim, A. K.; Novoselov, K. S. *Science* **2009**, 323 (5914), 610–613.
- (25) Balden, M.; Roth, J. *J. Nucl. Mater.* **2000**, 280 (1), 39–44.
- (26) Vietzke, E. *J. Nucl. Sci. Technol.* **2002**, 39 (4), 363–366.
- (27) Xiang, H. J.; Kan, E. J.; Wei, S. H.; Whangbo, M. H.; Yang, J. L. *Nano Lett.* **2009**, 9 (12), 4025–4030.
- (28) Gupta, A.; Chen, G.; Joshi, P.; Tadigadapa, S.; Eklund, P. C. *Nano Lett.* **2006**, 6 (12), 2667–2673.
- (29) Graf, D.; Molitor, F.; Ensslin, K.; Stampfer, C.; Jungen, A.; Hierold, C.; Wirtz, L. *Nano Lett.* **2007**, 7 (2), 238–242.
- (30) Wittmann, M.; Kupperts, J. *J. Nucl. Mater.* **1996**, 227 (3), 186–194.
- (31) Kupperts, J. *Surf. Sci. Rep.* **1995**, 22 (7–8), 251–321.

JA107071G